

## APPROXIMATE ANALYTICAL CALCULATION OF THE MACH CONFIGURATION OF STEADY SHOCK WAVES IN A PLANE CONSTRICTING CHANNEL

A. E. Medvedev and V. M. Fomin

UDC 533.601.15

*An approximate analytical model for calculation of the parameters of a steady gas flow inside a plane constricting channel formed by two symmetrically positioned wedges is suggested. A Mach configuration of shock waves (triple point) is formed in the channel when the wedge angles are larger than some critical value. The flow calculation in a constricting channel reduces to the solution of the iterative problem for a system of nonlinear algebraic equations. The configurations of shock waves, the slipstream, and the sonic line are described by the proposed model of a gas flow. A comparison of the results obtained using this model allows a fairly accurate calculation of the Mach stem and the length of the subsonic-flow region.*

Flow studies in constricting channels formed by two symmetrically positioned wedges have been performed owing to the interest in the problems of nonunique determination of the transition criteria from regular to irregular (Mach) reflection of an oblique shock wave from the symmetry plane [1–3]. Avoiding the problem of the choice of the critical angle of the wedge (the wedge angle is assumed to be larger than the critical value) and associated problems, we should note that the qualitative pattern of Mach reflection in the channel is not yet clear. An engineering approach [4, 5] gives good agreement with experimental results for the height of the Mach stem, but underestimates the length of the subsonic region behind the Mach stem since the model is approximate [2]. Li and Ben-Dor [6] analytically calculated the interaction of an expansion fan formed on the trailing edge of the wedge with the reflected shock wave and contact discontinuity. After that, the position of the throat of a one-dimensional nozzle is refined for calculation of the height of the Mach stem on the basis of the model [5].

We consider a plane channel formed by two symmetrically positioned wedges. A supersonic gas flow comes from the left. Since the problem is symmetric, we consider only the upper half-plane with the wedge ABG and the symmetry axis ON (Fig. 1). In Fig. 1, T is the triple point, AT is the attached shock wave, TO is the normal shock wave, i.e., the Mach stem, TF is the oblique shock wave, TE is the slipstream, GF is the first characteristic of the expansion fan, FE is the first characteristic of the expansion fan refracted on the shock wave TF, EN is the sonic line, and 1–4 are the gas-flow regions. The linear dimensions of the problem are the entrance half-section of the channel  $Y_1$ , the height of the Mach stem  $Y_m$ , the wedge length  $L$ , the distance  $Y_*$  from the axis of symmetry to the slipstream, the length  $L_*$  of the subsonic-flow region formed by the axis of symmetry and the contact discontinuity, between the normal shock wave TO and the sonic line EN, and the distance  $P$  between the shock wave TO and the trailing edge of the wedge BG ( $P > 0$  if the Mach stem is located downstream of the trailing edge of the wedge, otherwise  $P < 0$ ). The angular parameters of the problem are the wedge angle  $\theta$ , the angle of the attached shock wave  $\beta$ , the inclination angle  $\epsilon$  of the slipstream at the point T, the inclination angle  $\theta_T$  of the shock wave TF at the point T, and the angle  $\theta_F$  between the shock wave TF and the characteristic GF. In addition, the free-stream parameters, namely, velocity  $V_1$ , Mach number  $M_1$ , and pressure  $P_1$ , are known.

In accordance with Fig. 1, the model is based on the following assumptions.

---

Institute of Theoretical and Applied Mechanics, Siberian Division, Russian Academy of Sciences, Novosibirsk 630090. Translated from *Prikladnaya Mekhanika i Tekhnicheskaya Fizika*, Vol. 39, No. 3, pp. 52–58, May–June, 1998. Original article submitted September 30, 1996.

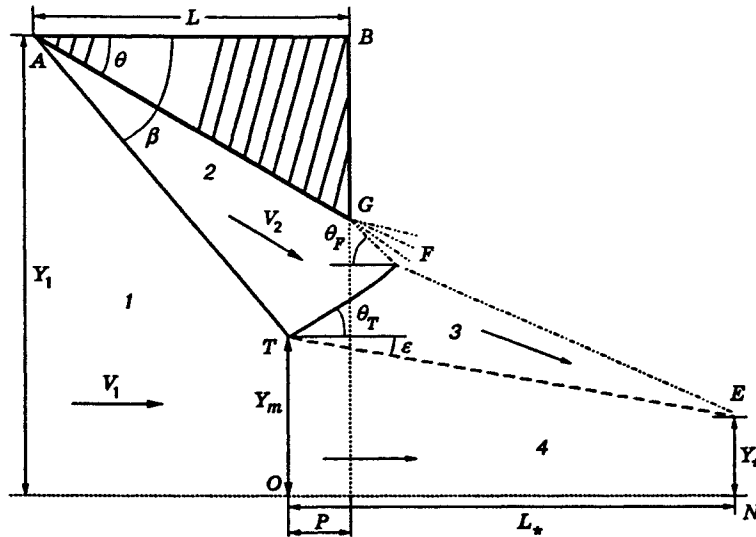


Fig. 1

(1) The wedge angle is larger than the critical value, and a configuration with the triple point T is formed; here the angle is  $\beta > \beta_N$ , where  $\beta_N$  is found from the equation [7]

$$\cot^4 \beta_N - \frac{\gamma \mu^2 (\xi + \mu^2) + (1 - \xi)^2}{(\xi + \mu^2)(1 + \xi \mu^2)} \cot^2 \beta_N - \frac{\gamma (\xi + \mu^2)}{(1 + \xi \mu^2)^2} = 0,$$

( $\mu^2 = (\gamma - 1)/(\gamma + 1)$ ,  $\xi = P_1/P_2$ ,  $\gamma$  is the ratio of the specific heats and  $P_1$  and  $P_2$  are the pressures upstream and downstream of the oblique shock wave AT, respectively).

(2) The wedge is rather short, and the wedge length  $L$  is such that the shock wave TF is not incident on the wedge side AG.

(3) The shock waves AT and TO are straight, the wave TF is curved, and the sonic line EN is straight.

(4) The first characteristic of the expansion wave FE crosses the slipstream TE at the point E of the sonic line EN.

Let the wedge (the length  $L$  and the angle  $\theta$ ) and the free-stream (the pressure  $P_1$ , the velocity  $V_1$ , and the Mach number  $M_1$ ) parameters be specified in region 1 (Fig. 1).

The solution in region 2 is found analytically from known relations [7]. The angle of inclination of the attached shock wave  $\theta$  is determined from the equation

$$\theta = \operatorname{arccot} \left\{ \left[ \frac{(\gamma + 1)M_1^2}{2(M_1^2 \sin^2 \beta - 1)} - 1 \right] \tan \beta \right\}. \quad (1)$$

The Mach number  $M_2$  and the pressure  $P_2$  are calculated from the formulas

$$M_2 = \sqrt{\frac{2 + (\gamma - 1)M_1^2}{2\gamma M_1^2 \sin^2 \beta - (\gamma - 1)} + \frac{2M_1^2 \cos^2 \beta}{(\gamma - 1)M_1^2 \sin^2 \beta + 2}}, \quad P_2 = \left[ \frac{2\gamma}{\gamma + 1} (M_1^2 \sin^2 \beta - 1) + 1 \right] P_1. \quad (2)$$

To find the angle  $\epsilon$ , we adopt the usual condition of equal pressures on both sides of the slipstream:

$$P_{30} = P_{40}.$$

Here  $P_{40} = \left\{ \left[ \frac{2\gamma}{\gamma + 1} (M_1^2 - 1) + 1 \right] P_1 \right\}$  is the pressure behind the shock wave TO in region 4, and  $P_{30} = \left\{ \left[ \frac{2\gamma}{\gamma + 1} (M_2^2 \sin^2 \beta_{23} - 1) + 1 \right] P_2 \right\}$  is the pressure behind the shock wave TF.

From here we find the angle between the shock wave TF and the velocity vector  $V_2$  at the point T:

$$\beta_{23} = \arcsin \left\{ \frac{1}{M_2} \sqrt{\frac{\gamma + 1}{2\gamma} \left( \frac{P_{30}}{P_2} - 1 \right) + 1} \right\}. \quad (3)$$

Then we have

$$\varepsilon = \theta - \operatorname{arccot} \left\{ \left[ \frac{(\gamma + 1)M_2^2}{2(M_2^2 \sin^2 \beta_{23} - 1)} - 1 \right] \tan \beta_{23} \right\}. \quad (4)$$

The angle  $\theta_T$  of TF inclination to the  $x$ -axis (at the point T) and the angle  $\theta_F$  between the first characteristic GF of the expansion wave and the  $x$  axis are as follows:

$$\theta_T = \beta_{23} - \theta, \quad \theta_F = \arcsin \frac{1}{M_2} + \theta. \quad (5)$$

We consider the gas-flow region TOEN (Fig. 1) within the framework of the model of a one-dimensional gas flow in a variable-section channel.

The gas flow behind TF in region 3 is supersonic. The gas flow in region 2 has no vortices; then, according to [8, 9], the flow in region 3 behind the shock wave TF (for a small curvature of TF, which will be shown below) remains vortex-free, i.e., potential. For such a flow, when the conditions on the characteristic FE and the contact boundary TE are set, an approximate analytical solution [10] based on Khristianovich's approximation [11] of the Chaplygin function is known.

For the solution of this problem in region 4, we have the following system of equations: the height of the Mach stem is

$$\frac{Y_m}{L} = \frac{1}{M_{40}} \left[ \frac{2}{\gamma + 1} \left( 1 + \frac{\gamma - 1}{2} M_{40}^2 \right) \right]^{(\gamma+1)/2(\gamma-1)} \frac{Y_*}{L} \quad (6)$$

and the channel length is

$$\frac{L_*}{L} = \left( \frac{Y_m}{L} - \frac{Y_*}{L} \right) \cot \varepsilon. \quad (7)$$

Having found the height  $Y_m/L$ , we determine the quantity  $P/L$ , as in [4], from the equation

$$\frac{P}{L} = \frac{(Y_t/L - Y_m/L) + (\tan \theta - \tan \beta)}{\tan \beta}, \quad (8)$$

where  $Y_t/L = Y_1/L - \tan \theta$ .

From the solution in region 4, we can find the coordinates of the slipstream TE

$$y/L = Y_m/L - (x/L) \tan \varepsilon \quad (9)$$

( $x$  is the distance from the point  $O$  along the symmetry axis),

the pressure on the TE

$$p = p^* \left[ \frac{2}{\gamma + 1} \left( 1 + \frac{\gamma - 1}{2} M_4^2 \right) \right]^{-\gamma/(\gamma-1)}, \quad (10)$$

where

$$p^* = P_{40} \left[ \frac{2}{\gamma + 1} \left( 1 + \frac{\gamma - 1}{2} M_{40}^2 \right) \right]^{\gamma/(\gamma-1)}$$

is the pressure on the sonic line EN;

the Mach number  $M_4$  in region 4 is found from the equation

$$\frac{y}{L} = \frac{1}{M_4} \left[ \frac{2}{\gamma + 1} \left( 1 + \frac{\gamma - 1}{2} M_4^2 \right) \right]^{(\gamma+1)/2(\gamma-1)} \frac{Y_*}{L}; \quad (11)$$

and the Mach number on the TE from the side of region 3

$$M_3^2 = \frac{2}{\gamma - 1} \left[ \left( \frac{p}{p_n} \right)^{(\gamma-1)/\gamma} - 1 \right]. \quad (12)$$

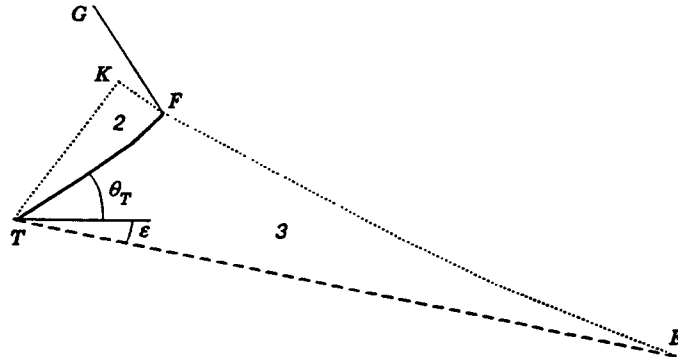


Fig. 2

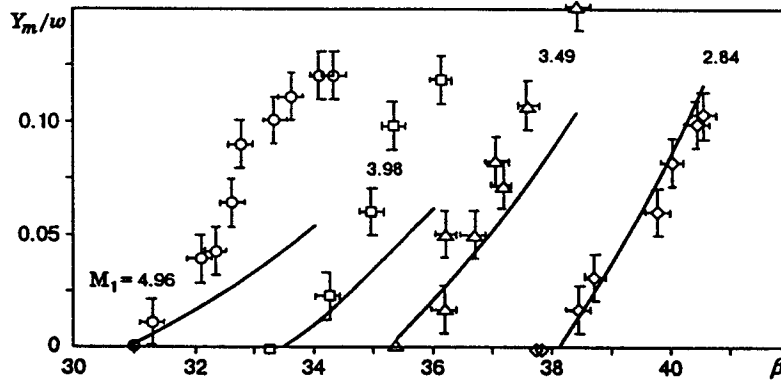


Fig. 3

Hère

$$p_n = P_{30} \left( 1 + \frac{\gamma - 1}{2} M_{30}^2 \right)^{\gamma/(\gamma-1)},$$

$$M_{30} = \sqrt{\frac{2 + (\gamma - 1)M_2^2}{2\gamma M_2^2 \sin^2 \beta_{23} - (\gamma - 1)} + \frac{2M_2^2 \cos^2 \beta_{23}}{(\gamma - 1)M_2^2 \sin^2 \beta_{23} + 2}}$$

is the Mach number behind the shock wave TF.

In region 3 we introduce the characteristic variables  $\xi$  and  $\eta$ :

$$\xi = 0.5(\tau + \vartheta), \quad \eta = 0.5(\tau - \vartheta),$$

where  $\tau = 1 - h \arctan(z/h) + \arctan z$ ,  $z = \sqrt{(\lambda^2 - 1)/(1 - \lambda^2/h^2)}$ ,  $h = \sqrt{(\gamma + 1)/(\gamma - 1)}$ , and  $\vartheta$  is the angle of inclination of the velocity vector to the  $x$  axis.

We consider the characteristic triangle TKE (Fig. 2) formed by the characteristics TK ( $\xi = \xi_1 = \text{const}$ ) and KFE ( $\eta = \eta_1 = \text{const}$ ). The functions  $\eta = \omega_1(\xi)$  and  $\xi = \omega_2(\eta)$  are determined on the line TE from Eqs. (9)–(11); then the equation for the slipstream TE is

$$x = x_1(\xi) = x_2(\eta), \quad y = y_1(\xi) = y_2(\eta). \quad (13)$$

The solution of the Cauchy problem for the region TKEF bounded by the characteristics TK and KFE and the streamline TE (slipstream) is given by the formulas [10]

$$x = \frac{\varphi(\xi) + \psi(\eta)}{\tan 2\xi + \tan 2\eta}, \quad y = \frac{-\tan 2\eta \cdot \varphi(\xi) + \tan 2\xi \cdot \psi(\eta)}{\tan 2\xi + \tan 2\eta}, \quad (14)$$

TABLE 1

$M_1$	$\beta$ , deg	$Y_m/w$	$Y_m/w$ (model [4])	Difference, %	$L_*/L$	$L_*/L$ (model [4])	Difference, %	$\bar{K}_{TF}$
5	31.0	0.0030	0.0029	3.45	0.2154	0.1910	12.77	0.0040
	32.0	0.0186	0.0180	3.33	0.2310	0.2049	12.74	0.0040
	33.0	0.0360	0.0349	3.15	0.2483	0.2203	12.71	0.0040
	34.0	0.0554	0.0539	2.78	0.2674	0.2375	12.59	0.0041
	35.0	0.0773	0.0754	2.52	0.2884	0.2565	12.44	0.0042
	36.0	0.1020	0.0998	2.20	0.3118	0.2777	12.28	0.0042
	37.0	0.1299	0.1275	1.18	0.3373	0.3013	11.95	0.0043
10	25.4	0.00075	0.0004	90.00	0.0830	0.0403	106.0	0.0030
	26.4	0.0058	0.0032	81.25	0.0978	0.0500	95.60	0.0031
	27.4	0.0122	0.0072	69.44	0.1117	0.0606	84.32	0.0032
	28.4	0.0201	0.0124	62.10	0.1274	0.0724	75.97	0.0032
	29.4	0.0297	0.0190	56.32	0.1444	0.0853	69.28	0.0032
	30.4	0.0409	0.0272	50.37	0.1620	0.0994	62.98	0.0033
	31.4	0.0542	0.0373	45.31	0.1815	0.1150	57.83	0.0034

where

$$\varphi(\xi) = \frac{[y_1(\xi) - \tan 2\xi \cdot x_1(\xi)][\tan 2\xi + \tan 2\omega_1(\xi)]}{-\tan 2\omega_1(\xi) - \tan 2\xi},$$

$$\psi(\eta) = \frac{[y_2(\eta) + \tan 2\eta \cdot x_2(\eta)][\tan 2\omega_2(\eta) + \tan 2\eta]}{\tan 2\omega_2(\eta) + \tan 2\eta}.$$

The system of nonlinear equations (1)–(14) yields a solution of the problem of determination of the flow parameters with the Mach shock-wave configuration shown in Fig. 1.

The shock wave TF (Fig. 2) is constructed under the condition of compatibility of the solutions in regions 2 and 3. The position of the curved shock wave TF is determined from the known velocity field in region 3 and initial angle of inclination  $\theta_T$  of the shock wave at the point T. A vortex flow is observed behind the curved shock wave TF. We determine the mean curvature  $\bar{K}_{TF}$  of the shock wave TF:  $\bar{K}_{TF} = L_{TF}/(2\pi \bar{R}_{TF})$ . Here  $L_{TF}$  is the length of the curve TF, and  $\bar{R}_{TF}$  is the mean (over the length of the curve TF) radius of the circumferences which have at least the second-order tangency with the curve TF at each point on TF. We note that  $\bar{K} = 0$  for a straight line and  $\bar{K} = 1$  for a circle.

Calculation results of the height of the Mach stem  $Y_m/w$  and the length  $L_*/L$  of the subsonic region 4, which were attained using our model and the model of [4], are listed in Table 1 for two values of  $M_1$  and various values of the angle  $\beta$  ( $Y_i/L = 0.37$  and  $\gamma = 1.4$ ). The last column gives the mean curvature  $\bar{K}_{TF}$  calculated using our model. It is seen that the mean curvature  $\bar{K}_{TF}$  of the shock wave TF is small. The main deviation from the angle  $\theta_T$  occurs near the point F. This is due to a drastic decrease in pressure at the slipstream TE near the sonic point E [8]. For a small curvature of the shock and a weak shock wave, according to [12] the flow vorticity behind the shock wave is a third-order quantity, as compared with disturbances of the gas velocity. Thus, the flow in region 3 can be considered vortex-free, i.e., potential, to a high accuracy.

Figure 3 compares experimental results [1] (points) and calculated data (curves) for the reduced height of the Mach stem; here  $w = L/\cos \theta$ . Experiments [1] and calculations were performed for  $\gamma = 1.4$  and  $Y_i/L = 0.37$ . The calculations by the model of [4] for these parameters (Fig. 3) yield very close results for the height of the Mach stem (see Table 1). The discrepancy between the results obtained using the present model and the model of [4] is observed in the values of the length  $L_*/L$  of the subsonic region 4, and the difference in the values of the height of the Mach stem is significant only at high Mach numbers.

A comparison of the calculation results obtained using the present model and the model of [4] showed (see Table 1) that, for moderate Mach numbers ( $M_1 < 10$ ), the difference in  $Y_m/w$  is as small as a few percent. The calculations by both models give close results if the initial conditions described in [1] are used. The difference in  $L_*/L$  for  $M_1 < 10$  is approximately 12%. For  $M_1 = 10$ , the difference in  $Y_m/w$  for these models is between 50 and 90%, and the difference in  $L_*/L$  is between 50 and 100%.

It is seen from the results of direct numerical simulation of the flow [2] in the geometry considered (see Fig. 1) that the length  $L_*/L$  is larger than that calculated by the model of [4] and is close to that calculated using our model.

A comparison with the experimental data of [1] (Fig. 3) demonstrated good agreement of the calculated and experimental data for  $M_1 = 2.84$  and  $3.49$ . For  $M_1 = 3.98$  and  $4.96$ , the results diverge as the angle  $\beta$  increases. This is caused by the approximate character of the proposed model: at large values of  $M_1$  one should take into account the nondimensionality of the gas flow in region 4 and the viscosity at the contact discontinuity TE (see Fig. 1). It is noteworthy that, for  $M_1 = 3.98$  and  $4.96$ , the height of the Mach stem predicted by the model that we presented is by 2–4% greater than that predicted by the model of [4].

## REFERENCES

1. H. B. Hornung and M. L. Robinson, "Transition from regular to Mach reflection of shock waves. Part 2. The steady-flow criterion," *J. Fluid Mech.*, **123**, 155–164 (1982).
2. M. S. Ivanov, S. F. Gimelshein, and A. E. Beylich, "Hysteresis effect in stationary reflection of shock waves," *Phys. Fluids*, **7**, No. 4, 685–687 (1995).
3. A. Chpoun and G. Ben-Dor, "Numerical confirmation of the hysteresis phenomenon in the regular to the Mach reflection transition in steady flows," *Shock Waves*, **5**, 199–203 (1995).
4. D. J. Azevedo and C. S. Liu, "Engineering approach to the prediction of shock patterns in bounded high-speed flows," *AIAA J.*, **31**, No. 1, 83–90 (1993).
5. D. J. Azevedo, C. S. Liu, and W. J. Rae, "Prediction of inviscid stagnation pressure losses in supersonic inlet flows," *AIAA J.*, **28**, No. 10, 1834–1836 (1990).
6. H. Li and G. Ben-Dor, "The wave configuration of a Mach reflection in steady flows: Analytical solution and dependence on downstream influences," in: Proc. 20th Int. Symp. on Shock Waves (Pasadena, July 23–28, 1995), pp. 77–78.
7. R. Courant and K. Friedrichs, *Supersonic Flow and Shock Waves*, Interscience, New York (1948).
8. L. G. Loitsyanskii, *Mechanics of Liquids and Gases*, Pergamon Press, Oxford-New York (1966).
9. N. E. Kochin, A. I. Kibel', and N. V. Rose, *Theoretical Hydromechanics* [in Russian], Part 2, Fizmatgiz, Moscow (1963).
10. A. A. Grib and A. G. Ryabinin, "Approximate integration of the equations of steady supersonic gas flow," *Dokl. Akad. Nauk SSSR*, **100**, No. 3, 425–428 (1955).
11. S. A. Khristianovich, *Continuum Mechanics* [in Russian], Nauka, Moscow (1981).
12. S. I. Pai, *Introduction to the Theory of Compressible Flow*, Van Nostrand, New York (1960).